Available online at www.sciencedirect.com
ScienceDirect
Ceramics International 34 (2008) 1173–1182
CERAMICS INTERNATIONAL
www.elsevier.com/locate/ceramint

Advanced indium-tin oxide ceramics for sputtering targets

E. Medvedovski [a,*], N. Alvarez [a], O. Yankov [a], M.K. Olsson [b]

[a] *Umicore Indium Products, 50 Sims Ave., Providence, RI 02909, USA*
[b] *Umicore Materials AG, Altelandstrasse 8, FL-9496 Balzers, Liechtenstein*

Received 14 July 2006; received in revised form 8 December 2006; accepted 12 February 2007
Available online 7 May 2007

Abstract

Indium-tin oxide (ITO) ceramic sputtering targets are widely used in formation of electrically conductive transparent thin films for electrodes in flat panel displays, solar cells, antistatic films and others, and which are commonly produced by a conventional dc magnetron sputtering process. The ceramic targets should be of high purity with a uniform microcrystalline structure and should possess high density and high electrical conductivity. In the present work, the challenges of the ceramic composition (e.g. the ratio of In_2O_3 and SnO_2) and manufacturing are considered; they include the use of high quality starting materials, particularly In_2O_3 powders with respect to purity, morphology and sinterability, manufacturing routes and sintering process. Positive experience in the development and manufacturing of ITO ceramic planar sputtering targets using in-house prepared In_2O_3 powders is reported. ITO ceramic tiles with areas up to 1500–1700 cm^2 and densities of 99+% of TD are manufactured. Physical properties of the ITO ceramics and sputtered films have been studied.

Keywords: A. Sintering; C. Electrical conductivity; Indium-tin oxide; Sputtering target

1. Introduction

Highly electrically conductive and transparent thin films are widely used as electrode layers in optoelectronic devices, such as in flat panel displays (FPD), e.g. liquid crystal displays (LCD), organic light-emitting diodes (OLED) and some others, solar cells, touch panels, electrochromic devices and antistatic conductive films [1–10]. The films are commonly produced by conventional dc magnetron sputtering on glass or polymer substrates, requiring a fine-tuned deposition process and high-quality sputtering targets. One of the most reliable and suitable materials, among different transparent conductive oxides (TCO), for sputtering targets is indium-tin oxide (ITO) ceramics. These ceramics are formed by the doping of some amounts of tin oxide to indium oxide, that results in modification (distortion) of crystalline lattice of indium oxide and in enhance its electrical conductivity. The ceramics should be of high purity with a uniform microcrystalline structure. They should possess high density (99+% of TD) to maximize the useful life of the targets and high electrical conductivity, and their use in sputtering system should provide a formation of crystalline or amorphous electrically conductive transparent films without structural defects. Due to the present need in large area optoelectronic devices with high-quality films, the ceramic targets are desirable to be as large as possible, i.e. dense monolithic tiles with areas up to 1500–1700 cm^2, which are used for assembling large-sized sputtering targets, are required. The manufacturing of these large-sized fully dense products is quite challenging for commercial ceramic processing.

Required electrical conductivity and transparency of ITO films are defined by compositional and structural features of the ceramics and by sputtering process parameters. Regarding ceramics, the structure of the crystalline lattice of In_2O_3 modified by the dopant and oxygen deficiency in the lattice have a high importance, i.e. the content of SnO_2, substitution of In^{3+} by Sn^{4+} in the cation sites (that results in the donation of free electrons to the lattice and provides n-type conductivity) and densification of ceramics are among crucial factors [8–10]. Due to the lattice defects caused by interstitial atoms or vacancies and oxygen deficiency, it is not straight forward to define theoretical density of ITO ceramics. For example, it is considered as 7.13–7.16 g/cm^3 for the ITO 90/10 ceramic compositions.

The quality of dc magnetron sputtered thin films is generally superior when the ceramic targets have higher density; also

---

[*] Corresponding author. Tel.: +1 401 215 1704; fax: +1 401 421 2419.
E-mail addresses: Eugene.Medvedovski@am.umicore.com, emedvedovski@shaw.ca, emedvedovski@cox.net (E. Medvedovski).

doi:10.1016/j.ceramint.2007.02.015

higher density targets enhance deposition rate [4]. Dense ceramic targets have higher resistance against sputtering erosion and nodules formation. In particular, nodules (“black spots”), which may be considered as indium sub-oxide, occur during the sputtering on the periphery of erosion race track of targets and tends to cause electrical arcing; they deteriorate properties of the films and should be periodically removed during processing. The nature of the nodules formation is complex, and its mechanism has not yet been completely understood [5–7]. However, based on the experimental results, the authors [4] noted that high ceramic target purity is not the major condition to attain the films with lower resistivity, i.e. ultrahigh purity grade targets would be only a small advantage of the film quality. Sputtering parameters may have a greater influence on the film quality [7].

One of the most widely used ITO compositions is 90/10 ITO, i.e. with an approximate wt.% ratio of 90/10 between In_2O_3 and SnO_2; this ceramic composition provides high-quality conductive and transparent films required for the optoelectronic applications. However, some other ITO compositions, such as 98/2, 97/3, 95/5, 80/20, can also be used in similar and other electronics devices.

The development and characterization of ITO and some other In_2O_3-based ceramics are under ongoing consideration of the ceramic manufacturers and the TCO users [1–10]. Despite the numerous studies, it is not enough data for the ceramics produced on the commercial basis. In the present work, the challenges of the ceramic composition and manufacturing of ITO sputtering targets are considered; they include the use of high-quality starting materials, especially In_2O_3 powders with respect to purity, morphology and sinterability, manufacturing routes and sintering process. A positive experience in the development and manufacturing of ITO ceramic planar sputtering targets using in-house prepared In_2O_3 powders has been achieved by Umicore Indium Products (UIP). ITO ceramic tiles with areas up to 1200–1700 cm^2 (with a variety of dimensions) and densities of 99+% of TD are currently manufactured. Properties of the ITO ceramics manufactured in the industrial conditions and the films obtained from these ceramics deposited by dc magnetron sputtering are reported.

2. Experimental

2.1. Starting materials and manufacturing

High purity commercially produced In_2O_3 and SnO_2 powders are used as the main starting materials for production of ITO ceramics. The In_2O_3 powders are manufactured by UIP using a proprietary process from pure indium via its acidation with subsequent neutralization and precipitation of $In(OH)_3$. Then the prepared $In(OH)_3$ is calcined at a proper temperature. Usually hydrochloric acid is used for acidation, and the In_2O_3 powders prepared via this route are denoted as type II. Each lot of starting In and prepared $In(OH)_3$ and In_2O_3 powders are qualified by chemical analyses and powder characterization. Properties of the processed powders are summarized in Table 1, and their typical particle size distributions are performed in Fig. 1. The In_2O_3 powders have cubic shape, and they are generally aggregated (Fig. 2). Properties of SnO_2 powders manufactured by other suppliers are also summarized in Table 1.

Starting materials are mixed and milled using a ball milling process based on the specially designed procedure. Water-based ceramic slurries (employing specially selected dispersing and binding agents) with workable viscosities and specific gravities are used for slip casting process. Depending on the size of the manufacturing bodies, casting is conducted at specific parameters, which have to be selected for each case. After gentle drying and dry state cutting (if required), “green” bodies are fired in the high-temperature electric kilns using specially designed kiln loading and firing conditions. The optimized firing cycle (firing temperature is below 1600 °C) and firing conditions provide practically full densification (up to 99.5% of TD). Then fired tiles are cut and ground with diamond tooling in order to provide precise dimensions, flatness and surface quality, which are required for the back face metallization, bonding and magnetron sputtering processes. For example, roughness of the ceramics R_a is attained to be not greater than 0.45 μm. It should be noted that a multi-step process control during powder preparation and ceramic manufacturing is maintained that provides high-purity and high-quality ceramic targets.

2.2. Sputtering

ITO films were deposited from ITO ceramic targets with dimensions of 381 mm × 127 mm × 6 mm cut from actually producing tiles onto glass substrates Corning No. 1737F using an industrial vertical planar dc magnetron sputtering system (LLS EVO II). The base pressure in the process module was below 5×10^{-5} Pa. Typically a power density of 3.1 W/cm^2 was applied during the sputtering runs. The sputtering pressure was in the range of 0.3–0.6 Pa that could be adjusted using a

Table 1
Properties of starting powders for ITO ceramics

Material	Purity (%)	Particle size distribution (μm)			Specific surface (BET) (m^2/g)
		d_{10}	d_{50}	d_{90}	
$In(OH)_3$	99.99	1–3	7–12	15–20	8–12
In_2O_3, type II	99.99	0.8–0.9	3-5	7-8	0.7–1.0
In_2O_3, type IIB	99.99	0.05–0.1	0.4–1.3	1–2	13–18
SnO_2	99.9	0.1–0.2	0.3–0.9	2–3	4–9
ITO slip	–	0.1–0.2	0.4–0.6	1.5–2.5	5–7

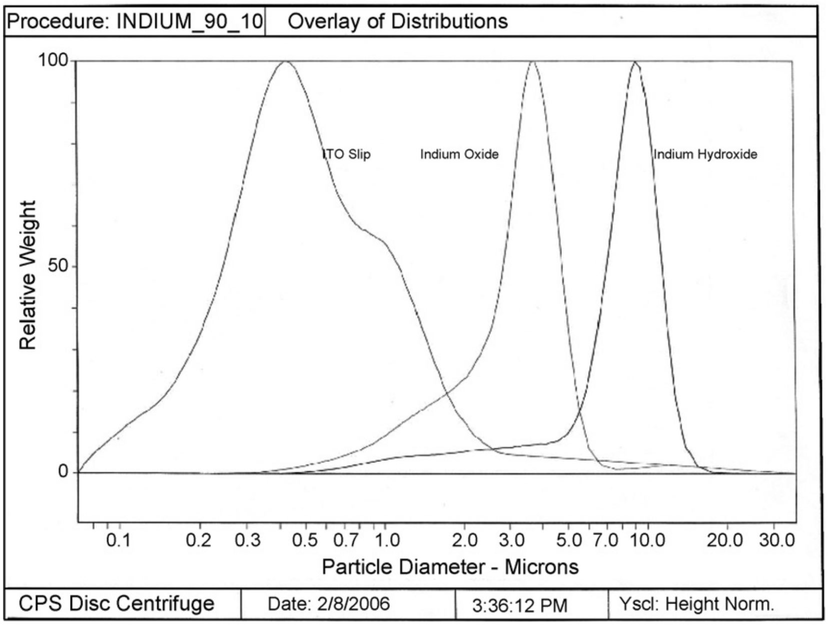

Fig. 1. Particle size distribution for $In(OH)_3$ and In_2O_3 powders and ITO slip.

mass flow controller. The sputtering process was run in Ar atmosphere with an addition of 0–5% of O_2 reactive gas. The sputtering runs were conducted at ambient and elevated temperatures (up to 200 °C); IR-radiation lamps installed in the process module were applied to maintain uniform substrate heating. Post-deposition heat treatment (annealing) of the coatings produced at ambient temperature was carried out using an electric furnace in air atmosphere. Annealing was carried out at temperature of 200 °C during 60 min. The parameters of the sputtering process were optimized in order to obtain high-quality films.

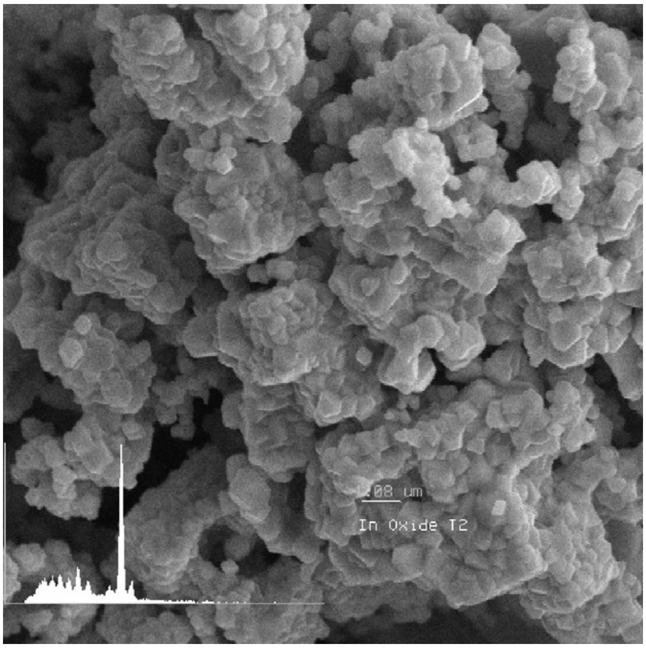

Fig. 2. SEM image of In_2O_3 type II powder.

2.3. Characterization

Powders were characterized for particle size distribution and specific surface using the Sedigraph and CPS Disc Centrifuge instruments and the Brunauer–Emmett–Teller (BET) method, respectively. The morphology of the powders was studied by high resolution scanning electron microscope (SEM). Phase composition and microstructure of the fired ceramics and sputtered films were studied using glancing incidence angle X-ray diffraction (XRD) and SEM and transmission electron microscopy (TEM) under different magnifications using "as-received" or etched samples. Thermal gravimetric analysis (TGA) was conducted in the range of 20–1400 °C using a standard procedure. Oxygen content in the ITO ceramics was determined using TGA. This method is based on the calculation of the weight decrease after reduction of the pulverized sintered ITO ceramic powder since it is assumed that the weight decrease is equivalent to the oxygen content in ITO when In and Sn are fully reduced.

Density of ceramic tiles was measured by the water immersion method based on Archimedes law. Young's modulus was tested using the resonant frequency method in accordance with ASTM C885. Sonic velocity was determined based on the formula connected Young's modulus and sonic velocity: $E = c^2 d(1 + p)(1 - 2p)/(1 - p)$, where E is Young's modulus, c is sonic velocity, d is density, p is Poisson ratio that is also determined by the ASTM 885. Flexural strength (four-point loading) was tested in accordance with ASTM C1161. Thermal diffusivity α was measured by the laser flash technique in accordance with ASTM E1461. Specific heat (heat capacity) C_p was tested using differential scanning calorimeter (ASTM E1269). Thermal conductivity λ values were calculated using a formula: $\lambda = \alpha C_p d$ (where d is density). Thermal properties were determined in the temperature range of 20–250 °C.

Coefficient of thermal expansion (CTE) was determined in the temperature range of 20–1000 °C using a quartz dilatometer. Specific electrical resistivity was determined using the four-point probe measuring unit. The test ceramic samples were cut from actual tiles-targets for the dimensions required by the appropriate testing procedures.

The ITO film thickness was optically determined using a J.Y. Horiba reflectometer analyzer. Specific electrical resistivity of the films also was determined using a Jandel four-point probe measuring unit. The transmittance in the visible range from 400 to 800 nm wavelength was measured using a Perkin Elmer optical analyzer. Film stress was determined for the selected films deposited onto Si wafers with 100 mm diameter using a standard procedure for flat panel displays using cantilever technique. The samples with deposited layers were undergone to the bending stress, and the bending contour was determined using an α-step profilometer.

3. Results and discussion

Basically, purity of ITO ceramics affects the quality of deposited films (their electrical conductivity and transparency) and sputtering process. The purity is defined both by the quality of starting materials and by the accuracy of the ceramic manufacturing. Indium oxide, as the major ingredient, should be used of 99.99%-purity based on total metallics. It is achieved by the accuracy and multi-step process control of In_2O_3 preparation.

The weight ratio between In_2O_3 and SnO_2 is selected in accordance with requirements of electrical properties of the ceramics and electrical properties and transmittance of the films. Based on numerous studies, the ratio of 90/10 generally provides the lowest electrical resistivity and high transmittance of the films prepared by sputtering techniques; however some other compositions may also be used for optoelectronic industrial specifications.

Slip composition of ITO ceramics is based on the optimal ratio between solid and liquid phases; the latter consists of water and the specially selected dispersants providing low viscosity with a relatively high specific gravity and a proper pH level. Based on the conducted studies focused on the selection of the dispersant and binder system with a proper pH level, the ITO slips have approximate solid contents of 80–84 wt.% (depending on the slip compositions).

In order to achieve a high level of homogenization of the ITO mix components and the slips and sinterability of the ceramics, wet mechanochemical activation processes have to be used. As noted, the starting powders should have low particle sizes and high specific surfaces that may be achieved either by the use of the as-prepared starting materials with required parameters (sub-micron particle size, etc.) or by the wet milling using properly selected grinding media and milling process. It is important due to the necessity to maintain an extremely low level of impurities, which may be introduced into ceramic mix during milling process (e.g. due to wear of grinding media and lining of the milling equipment). In order to achieve that, grinding media and lining should provide the highest wear resistance as possible, and the impurities incoming with the milling process should have a smaller effect on deterioration of sinterability of ITO and physical properties of sintered ceramics and deposited thin films. The optimized ball milling process provides particle size distribution and specific surface of the ITO slips, which are suitable for different types of ceramic processing using various sizes of moulds, even for the bodies with quite large dimensions, and to obtain adequate sinterability of the ceramics.

Densification of ITO ceramics depends on properties and morphology of starting materials, composition, e.g. a weight ratio of In_2O_3/SnO_2 in the mix, ceramic processing route and firing conditions. The ITO ceramic formation occurs via solid state sintering. SnO_2 may segregates preferentially around the voids in the interior of the sintered body, so it is desirable for better densification if SnO_2 particles are smaller as possible and if SnO_2 is well distributed between In_2O_3. It may be achieved by optimization of the mixing-milling process. The morphology of the starting powders affects the sinterability of ITO ceramics. It was found that if some amounts of In_2O_3 powder do not have a cubic shape due to some imperfectness of the In_2O_3 preparation, the ceramics have lower density. It is in a good correlation with the study conducted by Kim et al. [11], who found that the transformation of rhombohedral In_2O_3 to cubic induces coarsening of grains and formation of voids in microstructure retarding densification of the ceramics. In_2O_3-based ceramic compositions generally have a low sinterability. It is related to the partial dissociation and vaporization of In_2O_3 and SnO_2 at elevated temperatures in accordance with reactions [12–14]:

$$\begin{aligned}&In_2O_3(s) \rightarrow In_2O(g) + O_2(g) \quad (< 1300\,^{\circ}C),\\&In_2O_3(s) \rightarrow 2InO(g) + (1/2)O_2(g) \quad (> 1300\,^{\circ}C),\\&SnO_2(s) \rightarrow SnO(g) + (1/2)O_2(g)\end{aligned}$$

Partial vaporization of the oxides at elevated temperatures is confirmed by the results of TGA if the analysis is conducting at the lower oxygen environment (Fig. 3). Due to this fact, a temperature increase might not assist full densification if some conditions are not maintained. In order to achieve high densification (98+% of TD), hot pressing or an addition of sintering aids to the compositions or applying some other specific technological methods have to be used in order to modify firing process and to improve sinterability of ITO ceramics. Based on the conducted studies, a specially designed firing profile and oxygen-assisting firing conditions are used for sintering of the ITO ceramics. Density of ITO ceramic tiles fired in industrial conditions is achieved 7.12 g/cm^3 (90/10 composition), i.e. up to 99.5% of TD considering as 7.14 g/cm^3, with a good reproducibility. The density values strongly depend on the size of the tiles and the firing conditions. As the smaller the tiles dimensions, higher density of the tiles may be easier obtained. However, these high density values can be achieved not only for the tiles with areas of 500–900 cm^2, but also for the tiles with areas of up to 1200–1700 cm^2. Fired large tiles with the above mentioned values of density produced at UIP are demonstrated in Fig. 4. Compared to hot pressing, the using

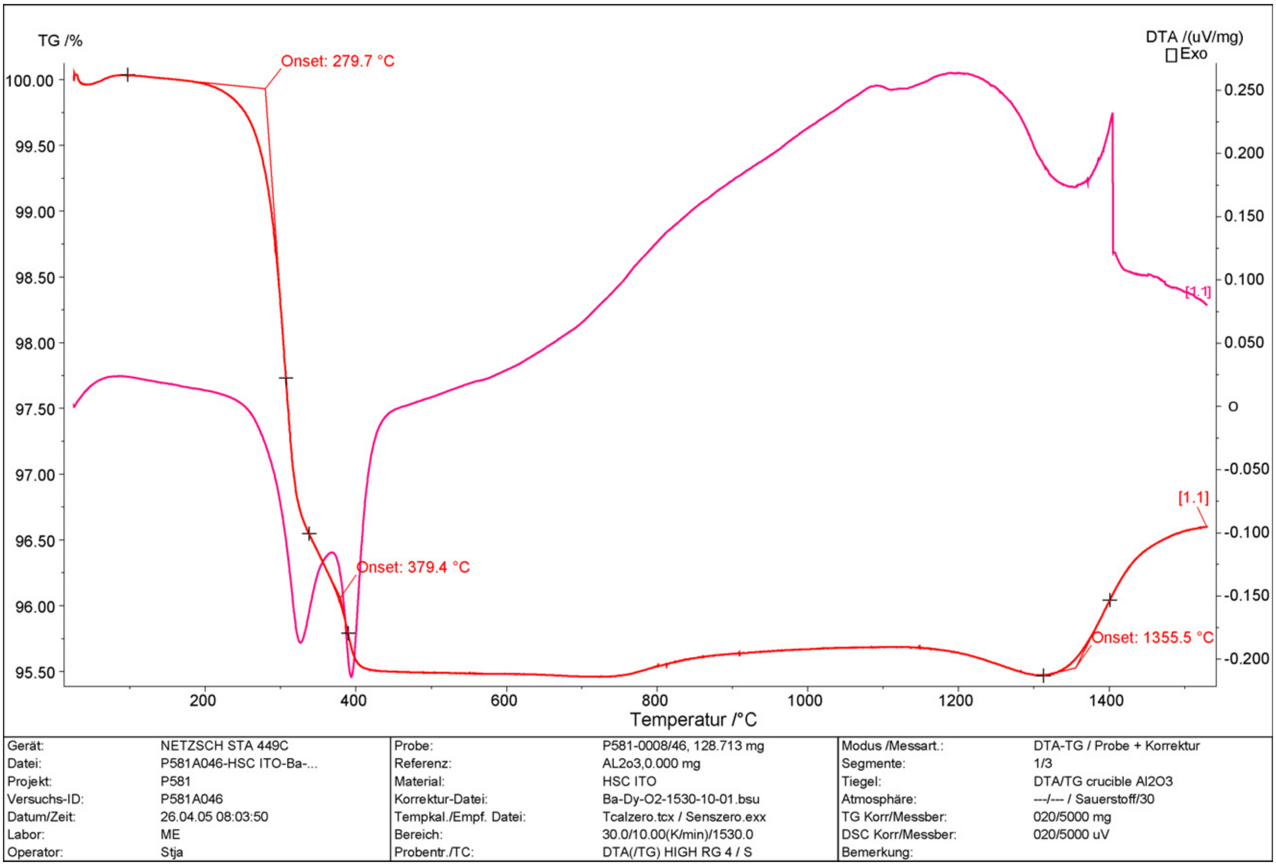

Gerät:	NETZSCH STA 449C	Probe:	P581-0008/46, 128.713 mg	Modus /Messart.:	DTA-TG / Probe + Korrektur
Datei:	P581A046-HSC ITO-Ba-...	Referenz:	AL2o3,0.000 mg	Segmente:	1/3
Projekt:	P581	Material:	HSC ITO	Tiegel:	DTA/TG crucible Al2O3
Versuchs-ID:	P581A046	Korrektur-Datei:	Ba-Dy-O2-1530-10-01.bsu	Atmosphäre:	---/--- / Sauerstoff/30
Datum/Zeit:	26.04.05 08:03:50	Tempkal./Empf. Datei:	Tcalzero.tcx / Senszero.exx	TG Korr/Messber:	020/5000 mg
Labor:	ME	Bereich:	30.0/10.00(K/min)/1530.0	DSC Korr/Messber:	020/5000 uV
Operator:	Stja	Probentr./TC:	DTA(/TG) HIGH RG 4 / S	Bemerkung:	

Fig. 3. TGA curve of ITO (90/10) ceramics.

firing conditions have valuable advantages with respect to lower cost of manufacturing equipment and lower running cost and greater capacities of the furnaces for mass production, including a possibility to fire large-sized products.

The use of In_2O_3 powders prepared by the alternative manufacturing routes may positively affect sinterability of ITO ceramics. However, such powders, due to their high specific surfaces and morphology features, may have unsatisfactory dispersability and may require a high amount of water for the preparation of slurries with adequate rheological properties. Hence, a compromise between sinterability of In_2O_3 powders and ability to prepare workable slips should be found. Thus, a small addition of such ‘‘fine’’ In_2O_3 powder in the ITO composition could provide a positive effect on sinterability of the ceramics that was confirmed by the density values and by increased values of fired shrinkage.

The ITO ceramics studied in this work have the major crystalline phase of In_2O_3 (bixbyite). However, XRD analysis indicates the presence of a secondary phase $In_4Sn_3O_{12}$ in ITO 90/10 and 80/20 ceramics that correlates with the literature data with respect to the presence of this phase in the ITO ceramics with a content of 6 at.% or more of Sn [15–17]. The content of this phase is a few percent (probably, not greater than 5–6%); however, this value is very approximate and not accurate. In many cases, the detection of this secondary phase is rather hard since its peaks on the diffractograms are overlapping with the peaks of the major In_2O_3 phase. The formation of this secondary phase may be considered as positive from the ITO ceramic densification standpoint because this new phase forming during sintering occupies the ‘‘space’’ between In_2O_3 grains. Due to the formation of the $In_4Sn_3O_{12}$ phase, it is much easier to obtain density values of 7.10–7.14 g/cm^3 for the 80/20 composition, although TD of this composition is lower. Crystallization of SnO_2 phase was not detected that is in agreement with other studies [5,13,15,16]. Microstructure of the ITO ceramics made by UIP is dense, rather uniform, and it consists of the grains with sizes of from 2 to 20 μm mostly with a cubic shape (Fig. 5), which consist of the crystallites with sizes of 25–45 nm. The sizes of crystallites were determined via XRD analysis using the Scherrer formula for calculation. Probably, a formation of the secondary phase promotes inhibition of the In_2O_3 grain growth that may be confirmed by the comparison of the grain sizes of the studied materials. As can be seen from SEM images, the grain sizes of ITO 95/5 ceramics are 10–20 μm (Fig. 5a), which does not contain the secondary phase, are larger than 90/10 (Fig. 5b) and 80/20

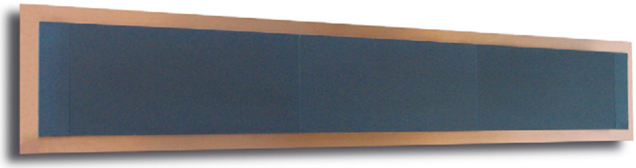

Fig. 4. ITO (90/10) sputtering target.

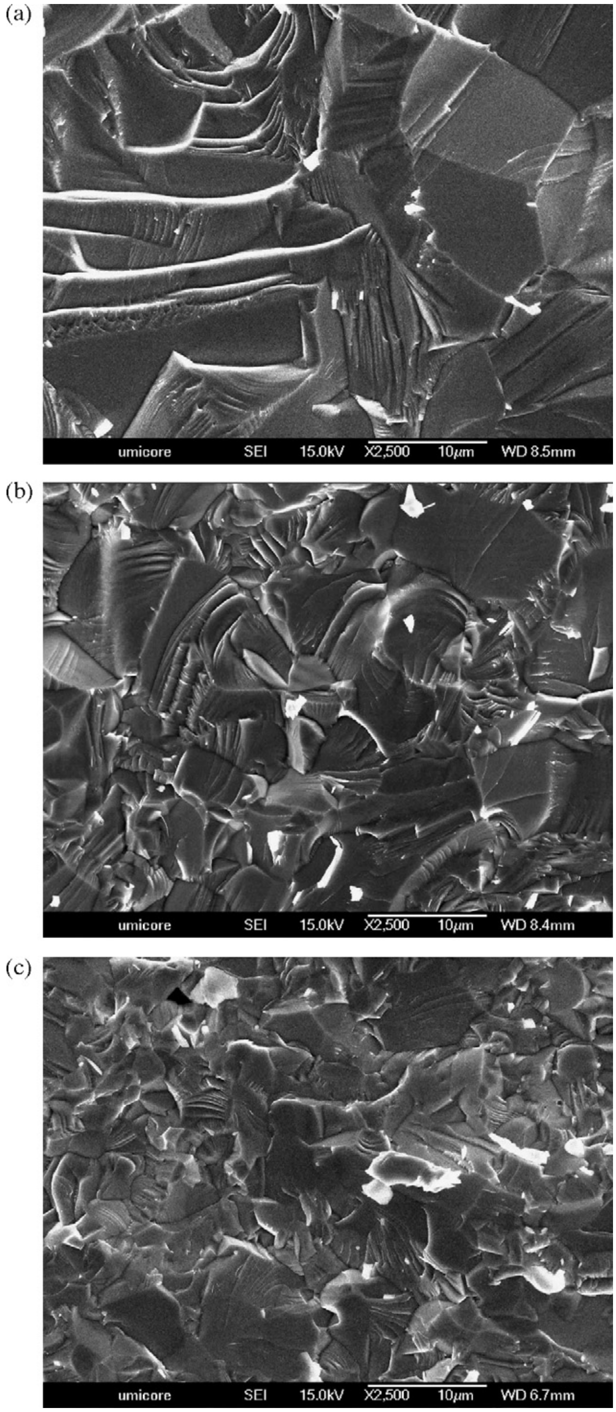

Fig. 5. Microstructure of ITO ceramics (SEM images): (a) 95/5; (b) 90/10; (c) 80/20.

(Fig. 5c) ceramics (grain sizes are 5–10 and 2–7 μm, respectively). The grains cleavage can be seen at the SEM images of the fracture of the samples that may be an evidence of a high densification of the ceramics since the fracture occurs through the grains. Irregular small intergranular pores are uniformly distributed, but they are not interconnected. It may be noted that, in the case of manufacturing of large-size products, the firing profile is usually extended in accordance with general principles of ceramics that results in more intensive grain growth.

A proper oxygen content of ITO targets is important for a stable sputtering process and for obtaining a wide ‘‘process window’’, that is desirable to be wider for consistency of the producing films. Depending on the process features, either fully oxidized or partially reduced ITO tiles are preferable. Theoretical oxygen content of ITO ceramics is not a reliable value because it depends on the method of calculation. This value may be 17.682% for the 90/10 composition if it is extracted from the mixture of 90 mass% In_2O_3 and 10 mass% SnO_2 or 17.243% if it is calculated from the composition $(In_{0.907}Sn_{0.093})_2O_3$, where some amount of Sn atoms substitute In atoms in the crystalline lattice. Due to the presence of a secondary $In_4Sn_3O_{12}$ phase, the oxygen content becomes even more uncertain. For our study, an oxygen content of 17.69% was considered as theoretical for the 90/10 composition, 18.08% for the 80/20 composition and 17.48% for the 95/5 composition. Oxygen content determination was conducted using a TGA analysis. The oxygen content of the studied ITO 90/10 ceramics is in the range of 17.55–17.90%, which is close to the theoretical value taking into account the measuring accuracy. In fact, the difference in actual and theoretical oxygen contents for the 80/20, 90/10 and 95/5 ITO compositions is higher for the compositions with lower In_2O_3 contents (for comparison, actual oxygen contents for 80/20 and 95/5 compositions are 17.94 and 17.43%, respectively). There is not a clear correlation between oxygen content values and densities of ITO ceramics when their densities are greater than 98.5–99% of TD. It is also hard to explain the variation in the values of oxygen content when the actual oxygen contents for some samples are even greater than the theoretical value. Probably, the answer has to be found in the consideration of the grain boundaries in ITO ceramics.

Physical properties of the ITO ceramics produced by UIP are performed in Table 2. Mechanical strength of these ceramics is on the moderate level; however, ITO ceramics are not intended for structural applications. Young’s modulus and sonic velocity, additionally to structural properties, indicate a ‘‘level’’ of densification, especially on the presence and quantity of closed pores and macrodefects, and their data may be useful for the comparison of the ceramics with the same composition, e.g. ITO materials. However, the determination of sonic velocity using the above mentioned formula may not be enough accurate for ITO ceramics because of relatively wide Poisson ratio variations for these materials.

The values of specific electrical resistivity of ITO ceramics are generally lower for the compositions of 90/10 comparatively with some other ITO compositions, e.g. they are ranging of $(1.3–1.7) \times 10^{-4}$ Ω cm for the compositions of 90/10 versus $(2.5–2.7) \times 10^{-4}$ and $(1.6–1.8) \times 10^{-4}$ Ω cm for the compositions of 80/20 and 95/5, respectively. However, the measure of electrical resistivity is not a 100% indicator of the ITO composition, especially if SnO_2 content is in the range of 5–12%. Densification of ITO ceramics has more influence on the electrical resistivity (the ceramics of the same composition but with higher density usually demonstrate lower values of specific electrical resistivity) than their ultrahigh purity. However, total high contents of impurities (such as more than

Table 2
Some physical properties of studied UIP ITO ceramics

Property	90/10	95/5	80/20
Density (g/cm^3)	7.07–7.12	7.07–7.12	7.07–7.14
Oxygen content (%)	17.55–17.90	17.40–17.46	17.90–17.97
Flexural strength (MPa)	150–180	–	–
Young's modulus (GPa)	160–190	–	–
Poisson ratio	0.285–0.335	–	–
Sonic velocity (km/s)	5500–6400	–	–
Specific electrical resistivity (Ω cm)	$(1.3–1.6) \times 10^{-4}$	$(1.6–1.8) \times 10^{-4}$	$(2.5–2.7) \times 10^{-4}$
CTE $\times 10^6$ (K^{-1})			
20–200 °C	7.0–7.5	7.0–7.3	7.4–7.6
20–700 °C	8.3–8.6	8.2–8.6	8.5–8.6
Thermal diffusivity (cm^2/s)			
20 °C	0.042–0.046	0.045–0.050	0.028–0.032
250 °C	0.034–0.038	0.038–0.042	0.024–0.026
Heat capacity (W s/g K)			
20 °C	0.36–0.37	0.36–0.37	0.36–0.37
250 °C	0.40–0.41	0.42–0.43	0.43–0.44
Thermal conductivity (W/m K)			
20 °C	11–12	12.5–13	8–8.5
250 °C	10–11	12–12.5	7.5–8

1000 ppm) may result in not only the undesirable distortion of the In_2O_3 crystalline lattice, but also in the formation of the electrically insulating layers between In_2O_3 grains, hence may enhance the ceramic electrical resistivity and, consequently, enhance the film resistivity. In this case, the consideration of impurities and their influence on electrical properties of the ITO ceramics should be ‘‘selective’’, e.g. the formation of alkali silicate or alkali earth silicate or some other glassy phases should be eliminated; at the same time, some other impurities do not affect electrical properties of ITO ceramics.

The values of electrical resistivity of ITO ceramics may vary in a rather wide range depending on the content of the lower conductive phase $In_4Sn_3O_{12}$. This phase, as shown above, is formed at the Sn content greater than 6%, and its content and a solubility of Sn in In_2O_3 may depend on the processing features, such as mixing-milling and, especially, firing conditions (e.g. temperature distribution in the kiln, oxygen level, etc.). Practically, oxygen level and sintering process also depend on the size of the ITO ceramic tiles, on their loading in the furnace and ‘‘thermal mass’’ of the ceramics (related to the tile sizes and amount of tiles in the furnace), which are varied from firing to firing in the manufacturing conditions. That is depending on these factors, the content of the forming $In_4Sn_3O_{12}$ phase and electrical conductivity of the ceramics may vary. Elevated values of electrical resistivity of the 80/20 composition are explained by the crystallographic structure of the material and a greater extent of the lower conductive $In_4Sn_3O_{12}$ phase. However, the presence of this $In_4Sn_3O_{12}$ phase positively affects density of ITO ceramics, i.e. the influence of the phase composition and structure of ITO ceramics on their properties and quality of the film is rather complex.

It is hard to correlate the influence of microstructure (grain size and grain size distribution) on electrical properties of ITO ceramics. There is no indication in literature regarding this influence, even for the small size samples processed and fired at very uniform laboratory conditions. Considering real production conditions, due to the variations in starting powders preparation and firing conditions, the structure may vary from firing to firing, especially if large-sized tiles are fired, and the influence of microstructure may be hardly observed. Only a small tendency of a conductivity increase with a grain size growth might be noticed.

Thermal diffusivity and thermal conductivity of ITO ceramics have to be higher as possible that is related with minimizing of thermal tensile stresses naturally occurring in the targets during sputtering; otherwise, related cracks may be a cause of non-uniform deposition of ITO films. The values of these properties are higher for the materials with higher contents of In_2O_3. The influence of ceramic densification on the thermal properties is similar to its influence on electrical conductivity; the higher the density, the greater the thermal diffusivity, the heat capacity and the thermal conductivity. The samples with higher electrical conductivity also demonstrate higher thermal conductivity. The values of thermal diffusivity and thermal conductivity decrease with a temperature increase, and the change of thermal conductivity versus temperature has a linear character, but the change of thermal diffusivity versus temperature does not have such behavior (Fig. 6). Both electrical and thermal conductivity are tend to be higher for the ITO samples with larger grain sizes; probably, it may be explained that if the ceramics have larger grains, less grain boundaries promote less resistance to electrical and thermal flows (with respect to electrical properties, this trend may be noted for the samples with significant difference in the grain sizes). The values of CTE of ITO ceramics with different contents of SnO_2 are on the same level that allows to use similar compositions for metallization and bonding processes of ITO targets.

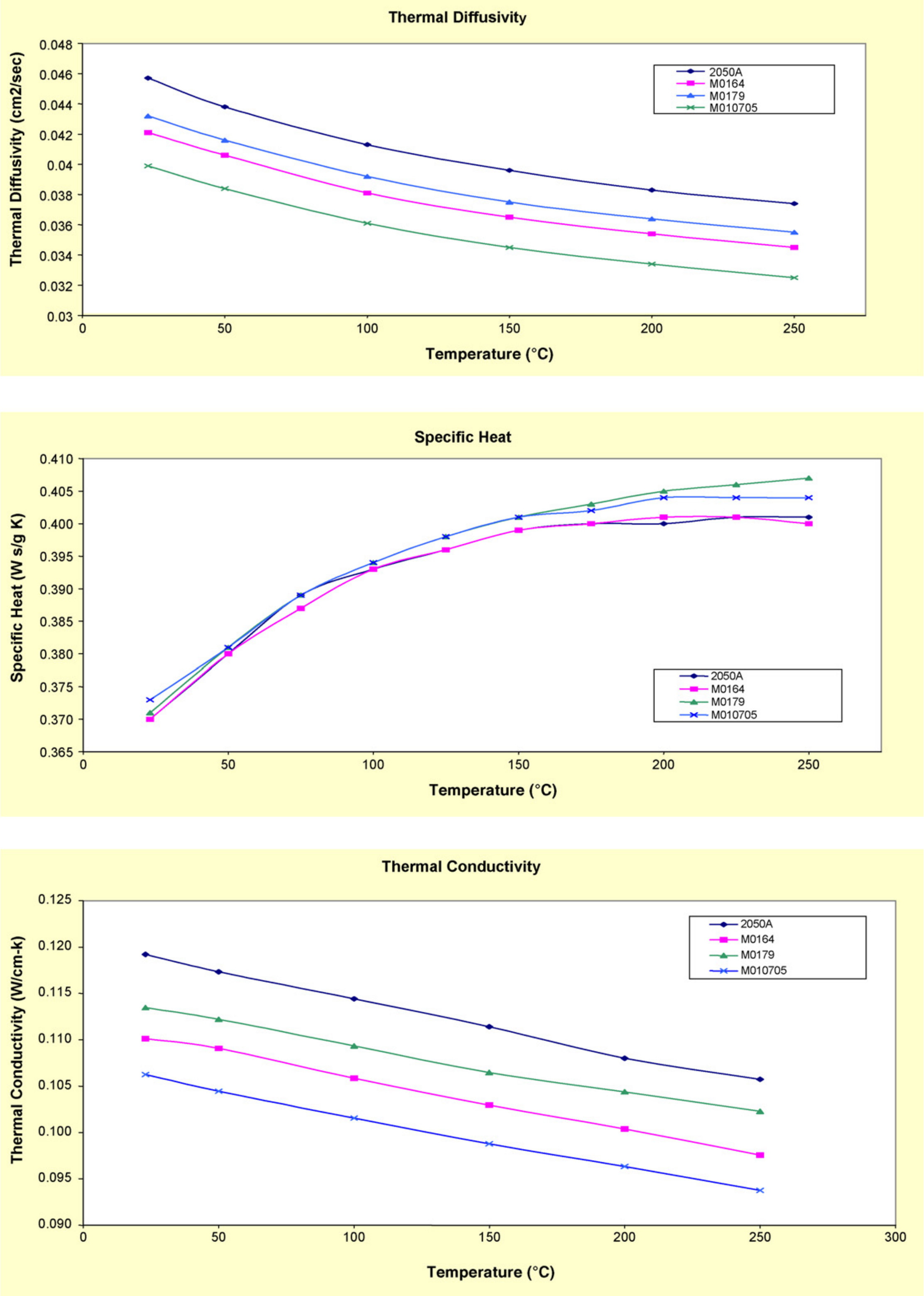

Fig. 6. Thermal diffusivity, heat capacity and thermal conductivity of ITO 90/10 ceramics.

Thin films with a thickness of 90–100 nm obtained by the conventional dc magnetron sputtering at different conditions were analyzed for their compositions, microstructure and physical properties. The study results for the films obtained from the targets made from 90/10 ITO ceramics as the most reliable composition are reported. By adjusting the amount of oxygen inserted to the system and some other sputtering parameters, a wide process ‘‘window’’, a stable sputtering process and high-quality layers were obtained.

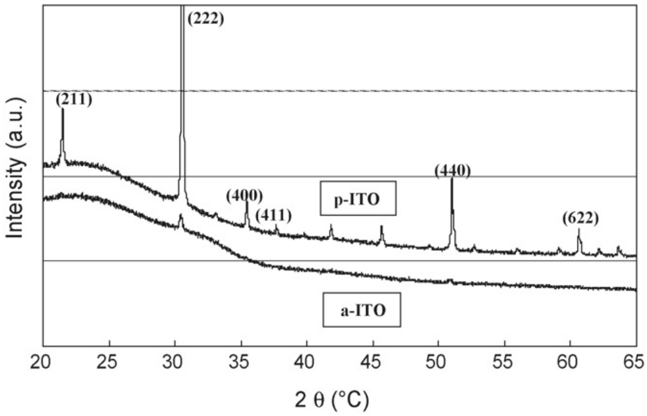

Fig. 7. XRD spectra of ITO (90/10) films obtained at different sputtering conditions (for amorphous and polycrystalline films).

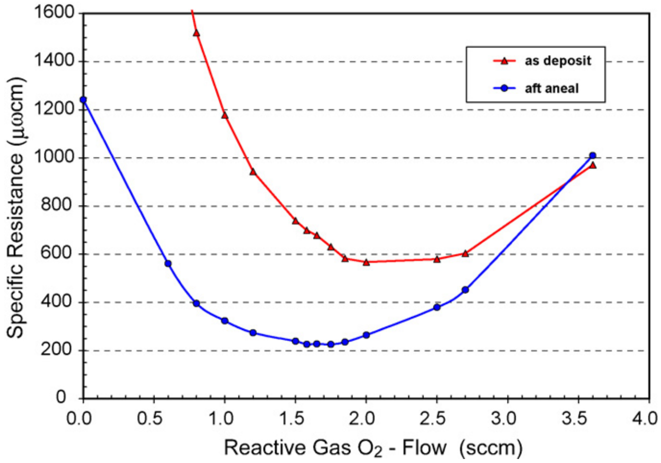

Fig. 9. Specific electrical resistivity of ITO films prepared from ITO 90/10 ceramic target by dc magnetron sputtering (after deposition and after annealing at 200 °C during 1 h).

The glancing incidence angle XRD spectra of selected ITO layer structures were recorded and compared with JCPDS database #6-0416. The spectrum of an almost entirely amorphous structure (a-ITO) with a small amount of crystalline sites was inherent to the ITO films deposited at room temperature (‘‘as-deposited’’) is demonstrated at Fig. 7. A polycrystalline structure (p-ITO) spectrum showing Bragg lines of the cubic In_2O_3 phase (Fig. 7) was related to the films produced with thermal activated processes. At low 2θ angles (20–35°), the signals from the layers are superimposed with X-ray amorphous spectrum of the glass substrate.

The morphology studies easily demonstrated the influence of sputtering conditions on the ITO film structures. The micrographs of a-ITO (‘‘as-deposited’’) films showed a poor contrast stemming. A polycrystalline structure of cubic shape In_2O_3 grains was inherent for the films deposited at elevated temperature of substrates. The films produced after annealing at 200 °C also had very homogeneous polycrystalline structures (p-ITO) consisted of the In_2O_3 phase. These crystalline structures had equiaxed (cubic) grains with average sizes of 10–25 nm densely packed (Fig. 8). Only occasional micropores might be observed at some triple junctions of the grains. The evolution of some columnar grown grains with a size of 30–50 nm to form larger domains may also be seen in Fig. 8. Such patterns are typical for heat treated and elevated temperature-deposited ITO films [18]. The conducted XRD and microstructure studies verified that the annealing process thermally activated a complete crystallization of the amorphous film structure and, subsequently, promoted a density increase of the ITO films.

Specific electrical resistivity of the amorphous (‘‘as-deposited’’) films was as low as about 600 μΩ cm at the oxygen flow of approximately 1.6% (Fig. 9). After annealing, specific electrical resistivity of the nanocrystalline ITO structures was lowered to 200–210 μΩ cm that is well accepted for various FPD applications. The transparency of the layers at 550 nm wavelength was approximately 85% with insertion of approximately 1.8% of oxygen for ‘‘as-deposited’’ films, while it was increased to more than 90% after 1 h annealing in air (Fig. 10). The results are in a good agreement with the previous

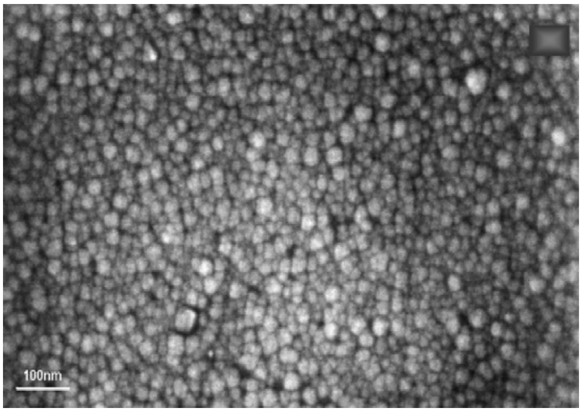

Fig. 8. Microstructure of ITO (90/10) film prepared by dc magnetron sputtering (deposition at room temperature with subsequent annealing at 200 °C during 1 h).

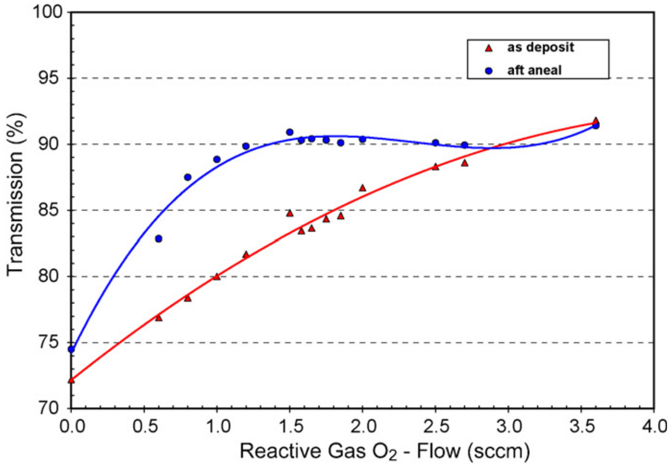

Fig. 10. Transmittance (at 550 nm wavelength) of ITO films prepared from ITO 90/10 ceramic target by dc magnetron sputtering (after deposition and after annealing at 200 °C during 1 h).

work [19] when an annealing process results in a relaxation of disorder bands as well as crystallization of the amorphous network, hence increasing electrical conductivity and optical transmittance of the layer. Deposition on the heated substrate provided obtaining of the same level of specific electrical resistivity and optical transmittance as the annealed layers due to the crystallization on the hot substrate.

The selected samples were evaluated with respect to their film stress. The ‘‘as-deposited’’ films are considered as being under compressive stress. The lowest value of approximately −200 MPa was measured. It was assumed that compressive of the ‘‘as-deposited’’ films stemmed mainly from the thermal expansion mismatch between ITO layer and the Si wafer substrate [19]. After the post-deposition annealing of the amorphous ITO film, the film stress converted from compression to tensile with a value of approximately +200 MPa. The transition of compressive stress of a-ITO to tensile stress of p-ITO after annealing may be due to an enormous densification of the amorphous structure transforming to the crystalline phase. Typically, the specifications for stress in ITO coatings for use in LCD industry are set at lower than ±500 MPa compressive/tensile [19], i.e. the obtained results are in a good agreement with industry requirements.

It was hard to define a strong correlation between density of ITO ceramics and macroscopic properties of the ITO films. Based on the studies conducted by Utsumi et al. [9], an increase of density of ITO ceramics from 90 to 99% of TD resulted in a slight decrease of the film resistivity due to a slight increase of the carrier concentration, and this change of resistivity was noted when density of ceramic samples increased from 97 to 99% of TD; however, there was not found an influence on transmittance of the films. However, it should be noted that all samples, which were undergone for the sputtering tests in the present work, had a high level of density (99% of TD or greater) that is required by the FPD industry. This high level of density of ceramics has to be maintained in order to achieve not only high quality of film properties, but also to minimize occurrence of the defects in the films and to maximize the sputtering efficiency in industrial conditions, especially in the case of the use of large area targets.

4. Conclusions

The developed technology of ITO ceramics using in-house prepared starting In_2O_3 powders allows to manufacture high-quality tiles with different dimensions and with the area up to 1700 cm^2 for planar sputtering targets. Fig. 4 illustrates a large target assembled from the UIP large center tiles (with a length of almost 500 mm) and smaller side tiles with an increased (15 mm) thickness, which is required for specific sputtering system applications. The manufactured ceramics have density up to 99.5% of TD for the products of various dimensions. Due to the selected compositions, high uniformity and densification, the obtained ceramics possess low electrical resistivity and acceptable structural and thermal properties. As a result, the dc magnetron sputtered films obtained with fine-tuned sputtering process parameters reveal low specific electrical resistivity and high transmittance required for applications in industrial large area and laboratory optoelectronic manufacturing.

Acknowledgements

The authors are grateful to Dr. G. Huyberechts (Umicore RDI, Belgium) for the helpful discussions and assistance in structural analyses. Assistance of Fraunhofer Institute for Thin Films and Surface Technology, FhG-IST Braunschweig (Germany) is appreciated greatly for conducting of XRD and high resolution SEM analysis of thin films.

References

[1] J.L. Vossen, Transparent conducting films, in: G. Haas, M.H. Francombe, R.W. Hoffman (Eds.), Physics of Thin Films, vol. 9, Academic Press, New York, 1977, pp. 1–71.

[2] D.S. Ginley, C. Bright, Transparent conducting oxides, MRS Bull. 8 (2000) 15–18.

[3] I. Hamberg, C.G. Granquist, Evaporated Sn-doped In_2O_3 films: basic optical properties and applications to energy-efficient windows, J. Appl. Phys. 60 (1986) R123–R160.

[4] B.L. Gehman, S. Jonsson, T. Rudolph, et al., Influence of manufacturing process of indium tin oxide sputtering targets on sputtering behavior, Thin Solid Films 220 (1992) 333–336.

[5] B.G. Lewis, R. Mohanty, D.C. Paine, Structure and performance of ITO sputtering targets, in: Proceedings of the 37th Annual Technical Conference, Society of Vacuum Coaters, Boston, MA, 1994.

[6] A.D.G. Stuwart, M.W. Thompson, Microphotography of surfaces eroded by ion bombardment, J. Mater. Sci. 4 (1969) 56–60.

[7] S. Ishibashi, Y. Higuchi, Y. Oka, et al., Low resistivity indium-tin oxide transparent conductive films. II. Effect of sputtering voltage on electrical property of films, J. Vac. Sci. Technol. A 8 (3) (1990) 1403–1406.

[8] G. Frank, H. Kostlin, Electrical properties and defect model of tin-doped indium oxide layers, Appl. Phys. A 27 (1982) 197–206.

[9] K. Utsumi, O. Matsunaga, T. Takahata, Low resistivity ITO film prepared using the ultra high density ITO target, Thin Solid Films 334 (1998) 30–34.

[10] P.A. Cox, W.R. Flavell, R.G. Egdell, Solid-state and surface chemistry of Sn-doped In_2O_3 ceramics, J. Solid State Chem. 68 (1987) 340–350.

[11] B.-C. Kim, S.-M. Kim, J.-H. Lee, et al., Effect of phase transformation on the densification of coprecipitated nanocrystalline indium tin oxide powders, J. Am. Ceram. Soc. 85 (8) (2002) 2083–2088.

[12] J.H.W. de Wit, The high temperature behavior of In_2O_3, J. Solid State Chem. 13 (1975) 192–200.

[13] J.H.W. de Wit, M. Laheij, P.E. Elbers, Grain growth and sintering of In_2O_3, J. Solid State Chem. 13 (1975) 143–150.

[14] R.H. Lamoreaux, D.L. Hidenbrand, L. Brewer, High-temperature vaporization behavior of oxides. II. Oxides of Be, Mg, Ca, Sr, Ba, B, Al, Ga, In, Tl, Si, Ge, Sn, Pb, Zn, Cd, and Hg, J. Phys. Chem. Ref. Data 16 (3) (1987) 419–443.

[15] J.L. Bates, C.W. Griffin, D.D. Marchant, et al., Electrical conductivity, seebeck coefficient and structure of In_2O_3–SnO_2, Am. Ceram. Soc. Bull. 65 (4) (1986) 673–678.

[16] N. Nadaud, N. Lequeux, M. Nanot, et al., Structural studies of tin-doped indium oxide (ITO) and $In_4Sn_3O_{12}$, J. Solid State Chem. 135 (1998) 140–148.

[17] T. Vojnovich, R.J. Bratton, Impurity effects on sintering and electrical resistivity of indium oxide, Am. Ceram. Soc. Bull. 54 (2) (1975) 216–217.

[18] M. Kamei, Y. Shigesato, S. Takaki, Origin of characteristic grain-subgrain structure of tin-doped indium oxide films, Thin Solid Films 259 (1) (1995) 38–45.

[19] U. Betz, M.K. Olsson, J. Marthy, et al., Thin films engineering of indium tin oxide: large area flat panel displays application, Surf. Coat. Technol. 200 (20/21) (2006) 5751–5759.